# A New Mouse Insertional Mutation That Causes Sensorineural Deafness and Vestibular Defects

**K. N. Alagramam,*[,1] H. Y. Kwon,[†,1] N. L. A. Cacheiro,[†] L. Stubbs,[‡] C. G. Wright,[§] L. C. Erway** and R. P. Woychik***

**Department of Pediatrics, Rainbow Babies and Children's Hospital, Case Western Reserve University, Cleveland, Ohio 44106, [†]Life Sciences Division, Oak Ridge National Laboratory, Oak Ridge, Tennessee 37831-8080, [‡]Human Genome Center, Lawrence Livermore National Laboratory, Livermore, California 94550; [§]Department of Otorhinolaryngology, University of Texas Southwestern Medical Center, Dallas, Texas 75235-9035 and **Department of Biological Sciences, University of Cincinnati, Cincinnati, Ohio 45221*

Manuscript received January 5, 1999
Accepted for publication April 22, 1999

ABSTRACT

This article describes a new recessive insertional mutation in the transgenic line *TgN2742Rpw* that causes deafness and circling behavior in mice. Histologic analysis revealed virtually complete loss of the cochlear neuroepithelium (the organ of Corti) in adult mutant mice. In association with the neuroepithelial changes, there is a dramatic reduction of the cochlear nerve supply. Adult mutants also show morphological defects of the vestibular apparatus, including degeneration of the saccular neuroepithelium and occasional malformation of utricular otoconia. Audiometric evaluations demonstrated that the mice displaying the circling phenotype are completely deaf. Molecular analysis of this mutant line revealed that the transgenic insertion occurred without creating a large deletion of the host DNA sequences. The mutant locus was mapped to a region on mouse chromosome 10, where other spontaneous, recessive mutations causing deafness in mice have been mapped.

INHERITED inner ear abnormalities in humans and mice can be grouped into several categories, including morphogenetic inner ear defects in which relatively gross changes in overall form of the labyrinth occur, cochleo-saccular defects involving disorders of inner ear fluid homeostasis, and neuroepithelial defects, in which the sensory epithelia are directly affected. Mutations with primary effects in the latter category are thought to be a major cause of inner ear defects in humans (Fraser 1976). Therefore, mouse mutants with neuroepithelial defects are potentially important models for such disorders in humans.

Neuroepithelial defects of the inner ear are often associated with partial or complete degeneration of the sensory neuroepithelia of the cochlea and/or the vestibular apparatus. The organ of Corti, as well as the maculae and cristae of the vestibular apparatus, may all be affected. The degenerative changes are due to primary disorders of the neuroepithelia, rather than being secondary to alterations in tissues that maintain homeostasis of the inner ear fluids. As a consequence of the sensory cell loss that occurs in these disorders, neural degeneration is usually also seen. In mice, this type of inner ear pathology is associated with several recessive mutations. These mutants often show the deafness and balance disturbances that frequently result from inner ear dysfunction (Steel 1995).

The inner ear is a complex organ in terms of its development, morphology, and function. As many as a hundred genes have been implicated in nonsyndromic hearing loss in humans (Morton 1991). In mice, the number of loci associated with hearing loss is thought to be >60 (Nadeau *et al.* 1991). Genes associated with the *shaker-1* locus (Gibson *et al.* 1995) and the *Snell's waltzer* locus (Avraham *et al.* 1995) were among the first two murine genes associated with deafness to be identified. While a few of the genes associated with human deafness have been cloned, many are yet to be identified (Van Camp and Smith). Some of the human genes associated with deafness have been identified recently through the analysis of mouse mutants. For example, neuroepithelial defects in the *shaker-1* mouse are caused by a mutation in the myosin VIIA gene (*Myo7a*; Gibson *et al.* 1995). A mutation in the human homologue, *MYO7A*, is involved in Usher syndrome 1B (congenital balance and hearing loss coupled with progressive retinitis pigmentosa; Weil *et al.* 1995), as well as nonsyndromic deafness (Liu *et al.* 1997; Weil *et al.* 1997). Similarly, the gene causing neuroepithelial defects in the mouse *shaker-2* locus was recently identified as coding for an unconventional myosin (*Myo15*; Probst *et al.* 1998), and the human homologue (*MYO15*) mapped to the nonsyndromic deafness locus *DFNB3* (Wang *et al.* 1998).

In humans, nonsyndromic deafness is more common than syndromic deafness (Schuknecht 1993). Among

*Corresponding author:* Richard P. Woychik, Parke-Davis Laboratory for Molecular Genetics, 1501 Harbor Bay Pkwy., Alameda, CA 94502. E-mail: rick.woychik@wl.com

[1] These authors contributed equally to this work.

the prelingual forms of deafness, autosomal recessive nonsyndromic deafness accounts for ~85% of the cases (Kalatzis and Petit 1998). Furthermore, the autosomal recessive forms of hearing loss are often more severe (compared to autosomal dominant or X-linked forms) and are almost exclusively sensorineural, due to defects in the cochlea (Schuknecht 1993; Kalatzis and Petit 1998). Therefore, characterization of a new mouse mutation causing nonsyndromic, recessive neuroepithelial deafness will be useful for studying this form of inner ear defect. Here we report the identification of such a mutation, the recessive insertional mouse mutation in the transgenic line *TgN2742Rpw* that exhibits auditory and vestibular defects associated with the inner ear neuroepithelium. Additionally, we provide evidence that the organ of Corti develops normally in the mutant mice and subsequently undergoes degeneration, and we describe the molecular characterization and mapping of the mutant locus to mouse chromosome 10. These studies suggest a potential relationship between our new mutant and other deafness mutations that have been mapped to the central region of chromosome 10. On the basis of its phenotype, the *TgN2742Rpw* transgenic mutant strain provides an excellent model for studies of nonsyndromic human deafness.

## MATERIALS AND METHODS

**Mice:** The transgenic line *TgN(Imw)2742Rpw* was generated as part of an insertional mutagenesis program in the Life Sciences Division at the Oak Ridge National Laboratory. Transgenic mice were generated by microinjection of an 8-kb linearized plasmid construct containing a rat lectin cDNA under the control of the human β-actin promoter into fertilized mouse embryos from the FVB/N strain. The transgenic line was generated and maintained in the FVB/N strain; this strain was used for all experiments described in this article.

**Identification of transgenic mice:** Genomic DNA from tail biopsies was isolated and quantified by fluorometry, and equal amounts of DNA were digested with *Eco*RI. The digested DNA was size fractionated on 0.8% agarose gels and Southern blotted to GeneScreen nylon membrane (Ausubel *et al.* 1991). Mutant mice were identified by hybridization to sequences from within the transgene. Initially, quantitative Southern analysis was used to distinguish heterozygotes from homozygotes. Later, when unique copy-flanking sequences were cloned (End-clone A and B, Figure 4A), these sequences were used to confirm the recessive nature of the *TgN2742Rpw* mutation: mice that showed the phenotype were homozygous for the transgene (Tg/Tg), and mice that were normal were either heterozgous for the transgene (Tg/+) or wild type (+/+).

**Histological analysis:** Morphological studies involved histological examination of inner ear cross-sectional anatomy utilizing specimens embedded in glycol methacrylate. Five wild-type adult (FVB/N) mice and five adult mutant mice were prepared for histological studies. Tissue specimens from all mice were processed as follows. The inner ear was fixed by perilymphatic perfusion of 2.5% phosphate-buffered glutaraldehyde. After several days in fixative, the temporal bones were decalcified in 0.35 m EDTA and embedded in glycol methacrylate resin. They were then sectioned at 2–5 μm and the sections stained with toludine blue for light microscopic study. Using this method, each temporal bone provided a series of sequential sections that included the full extent of the cochlea and vestibular apparatus. The mice used for histological analysis were between 10 and 12 mo old. Results from mutant mice were always compared to results obtained from wild-type littermates.

**ABR and behavioral testing:** Auditory function was evaluated by performing auditory-evoked brain stem response (ABR) tests. For our experiments, ABR responses were obtained according to the methodology described previously (Erway *et al.* 1993). In brief, acoustic stimuli were presented (20/sec) to the external auditory canals of anesthetized mice. Each stimulus elicits, from a normal ear, a volley of action potentials over the auditory nerve with subsequent activation of auditory centers in the brain stem. The brain stem responses (ABRs) from these stimuli were averaged from 128 to 1024 repetitions of the stimulus. Mouse ABR recordings exhibit four or five peaks, each with a well-defined latency (1–6 msec) and amplitude (1–10 μV). The threshold for the ABR was determined for clicks and puretone pips of 8, 16, and 32 kHz.

Vestibular function was evaluated by performing a swim test. The mice were placed in a clear plastic mouse cage half-filled with warm (30–35°) water. While in the water the mice were observed to determine if they showed "normal" swimming behavior. Normal swimming behavior is defined as follows: after being placed in water, wild-type mice quickly resurfaced with a "whipping" motion of their tails, managed to keep their noses and tails above the surface of water, and swam toward the side of the cage.

**Cloning the transgene insertion site:** Sequences flanking the transgene insertion site were identified using a plasmid rescue procedure that was originally used for cloning the *limb deformity* locus (Woychik *et al.* 1985). For the plasmid rescue procedure, we used a modified version of the cosmid vector c2RB (Bates and Swift 1983), where the $amp^R$ gene on the cosmid vector was inactivated, to generate a cosmid library of partial Sau3A genomic fragments. The library was screened by plating on medium containing ampicillin (Sambrook *et al.* 1989). Cosmid clones that grew on ampicillin plates were those with an insert containing the $amp^R$ gene derived from the integrated transgene. The presence of the transgene within the $amp^R$ clones was confirmed by hybridization with a radiolabeled probe corresponding to the transgene sequence. The host flanking sequences were identified by hybridization with a radiolabeled probe composed of total mouse genomic DNA (Woychik *et al.* 1985). Of these $amp^R$ clones, some contained only a portion of the transgene, while others contained a portion of the transgene along with sequences flanking the transgene integration site. One such clone, labeled cosmid-9, was analyzed further. The genomic fragment in cosmid-9 was screened for unique sequences (single-copy sequences devoid of any repetitive sequences/elements) by isolating several different restriction fragments and testing each of those fragments by hybridization to a Southern blot containing wild-type mouse genomic DNA. One such unique sequence, F9, hybridized to a unique band in wild-type DNA.

To clone the wild-type region corresponding to the mutant locus, probe F9 was used to screen a wild-type mouse genomic bacterial artificial chromosome (BAC) library according to the protocol supplied by Research Genetics (Birmingham, AL). End-cloning of the BAC insert was done as described previously (Ausubel *et al.* 1991). One end-clone fragment was called "end-clone A" (closer to the T7 site on the vector) and the other was referred to as "end-clone B" (closer to the SP6 site on the vector). The size of each end-clone was ~0.6 kb.

**Long-range restriction fragment analysis:** Genomic DNA was prepared from spleen cells derived from wild-type, heterozygous, and homozygous mice as described previously (Stubbs

**TABLE 1**

**Description of mapped gene markers and variant fragments**

| Gene symbol | Probe/type | Reference and/or source | Enzyme | Variant fragment sizes (C3Hf/*M. spretus*) |
|---|---|---|---|---|
| *Myb* | Mouse/cDNA | Mucenski *et al.* (1991) | *Taq*I | 3.1 kb/4.4 kb |
| *Cdc2a* | Mouse/cDNA | I.M.A.G.E. clone #387172 | *Taq*I | 7 and 4.8 kb/7.5 and 4.7 kb |
| *TgN2742Rpw* | Tg2742-4.5RI/genomic | This study | *Taq*I | 3.2 and 1.9 kb/5.5 kb |
| *Bcr* | Mouse/cDNA | I.M.A.G.E. clone #390100 | *Taq*I | 4 kb/4.4 kb |
| *Pfkl* | Human/genomic | Levanon *et al.* (1989); ATCC #63056 | *Eco*RI | 2.6 kb/4.2 kb |

*et al.* 1990). The genomic DNA was restriction digested for 12–15 hr with rare cutting enzymes under conditions suggested by the manufacturer (New England Biolabs, Beverly, MA). The protocols for pulsed-field gel electrophoresis (PFGE), Southern blotting, probing, and washings were carried out as described previously (Stubbs *et al.* 1994).

**Interspecific backcross mapping:** Southern blots carrying restriction-digested DNA from 160 interspecific backcross progeny (IB;C3Hf/Rl-*Mgf*$^{Sl2ENURg}$/+ × *Mus spretus*) × C3Hf/Rl; Stubbs *et al.* 1996) were prepared, and the blots hybridized with radiolabeled probes as previously described (Stubbs *et al.* 1990). Probes representing the *Cdc2a* and *Bcr* loci were cDNA clones identified by searching the dBEST database (Bouguski *et al.* 1993) for mouse expressed sequence tags (ESTs) that matched published sequences of the two genes most closely linked to the mutant region (mouse *Cdc2a*, Genbank accession no. M38724; Human *BCR* cDNA, Genbank accession no. U0700). The cDNA clones were obtained from the I.M.A.G.E. consortium collection through Research Genetics, Inc. (Huntsville, AL). The *Pfkl* cDNA was obtained from the American Type Culture Collection [(ATCC), Rockville, MD]. The mouse *Myb* cDNA was kindly provided by Dr. Michael Mucenski. Data were stored and analyzed and standard errors calculated using the Map Manager data analysis program (Manly 1993). Probes representing other Mmu10 gene markers and information regarding variant fragments that were used to follow their segregation are summarized in Table 1.

## RESULTS

**Generation of the *TgN(Imw)2742Rpw* mutant line:** We identified a new recessive insertional mutation in mice that confers a deafness and a circling phenotype. This mutation is designated as *TgN(Imw)2742Rpw* (Im, insertional mutation; w, waltzer), in accordance with standard nomenclature rules (Gordon 1992), and will be abbreviated as *TgN2742Rpw*. The transgene in the *TgN2742Rpw* line, which is composed of a rat lectin cDNA under the control of the human beta-actin promoter, segregates in a simple Mendelian fashion. Mice heterozygous for the transgene in this line are phenotypically normal. Of the offspring, ~25% arising from a cross between heterozygous transgenic parents develop the phenotype, and these progeny are all homozygous for the transgene (data not shown). Cytogenetic analysis of a homozygote and a heterozygote showed no detectable chromosomal abnormality, indicating that no gross chromosomal structural alterations have occurred in the *TgN2742Rpw* line (data not shown). On the basis of the recessive genetics of the mutant trait, coupled with the fact that none of the numerous other lines that have been prepared with the same transgene DNA construct showed a deaf-circling phenotype, we conclude that the phenotype in the *TgN2742Rpw* line arose from a mutation caused by the integration of the transgene sequences into the host genomic DNA.

**Histological examination:** Histological examination of inner ear specimens from adult mutant mice showed inner ear abnormalities affecting both the cochlear and vestibular portions of the membranous labyrinth. Analysis of homozygotes at ~1 yr of age revealed that the organ of Corti is almost entirely missing throughout all cochlear turns; that is, in most areas no inner or outer hair cells or supporting cells are present (Figure 1, A–D). However, as illustrated in Figure 1D, scattered remnants of the organ of Corti are occasionally noted and these are most often present in the apical cochlear turn. In areas where some sensory epithelium remains, recognizable fluid spaces can be seen within the organ of Corti. The spiral ganglion shows severely reduced numbers of neurons, which probably reflects ganglion cell degeneration secondary to loss of the inner hair cells. Although scattered strial atrophy affecting primarily the apical cochlear turn has been noted, the stria vascularis in these mutants appears mostly normal. In addition, Reissner's membrane and the membranous wall of the saccule are in normal positions.

The *TgN2742Rpw* mutant mice also show vestibular abnormalities, including degeneration of the saccular neuroepithelium and occasional malformation of utricular otoconia. In adult mice, the neuroepithelium of the saccular macula is completely absent, with no recognizable hair cells or supporting cells (Figure 2, A and B). The neuroepithelia of the utricle and semicircular ducts appear normal. However, sparsely distributed abnormally large otoconia have been noted overlying the utricular macula in some specimens (Figure 2, C and D).

**ABR and behavioral analyses:** We initially observed that the mutant mice did not respond to sharp metallic sounds, which suggested that they have impaired hearing ability. To quantify their auditory function, ABR was evaluated as described previously (Erway *et al.* 1993).

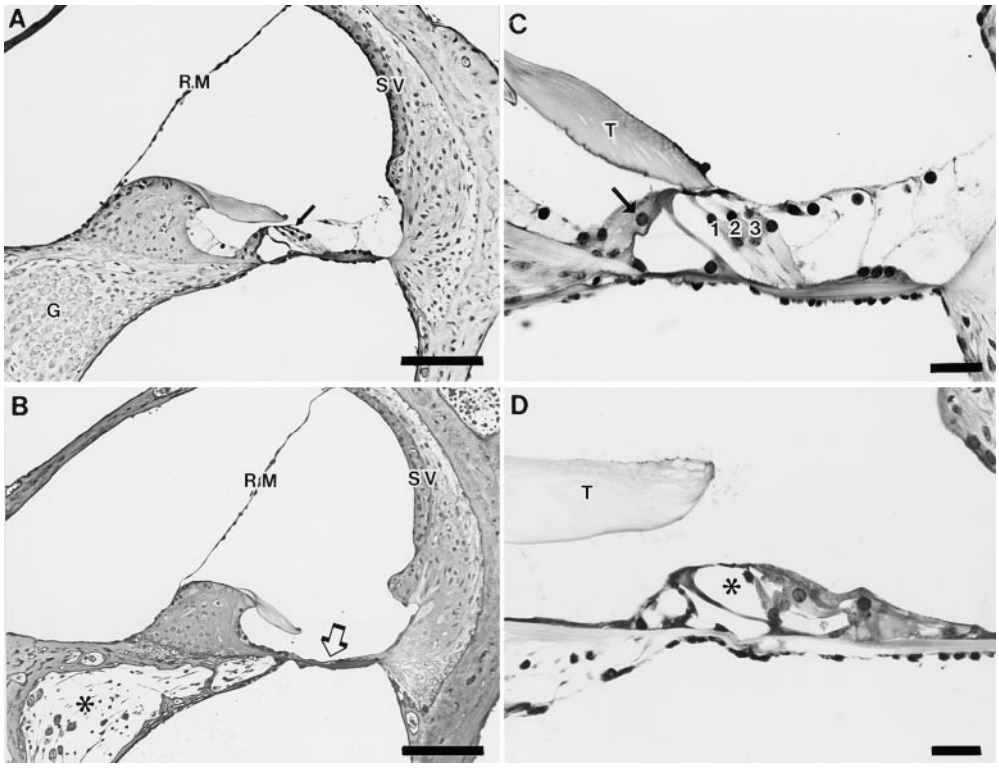


Figure 1.—Histological analysis of the cochlea from normal and *TgN2742Rpw* mutant mice at ~1 yr of age. (A) Low-power view of normal mouse cochlear duct in the upper basal turn showing major anatomical features: Reissner's membrane (RM), stria vascularis (SV), organ of Corti (arrow), spiral ganglion (G). Bar, 100 μm. (B) Low-power view of cochlear duct in the upper basal turn from an adult *TgN2742Rpw* mutant. Reissner's membrane (RM) and the stria vascularis (SV) appear normal; however, the organ of Corti is entirely absent (arrow) and the spiral ganglion (asterisk) shows a greatly reduced neuronal population. Bar, 100 μm. (C) Normal mouse organ of Corti in the upper basal turn illustrating the two types of auditory sensory cells: inner hair cells (arrow) and three rows (1,2,3) of outer hair cells with underlying supporting cells. T, tectorial membrane. Bar, 50 μm. (D) Degenerating organ of Corti in the apical cochlear turn of a *TgN2742Rpw* mutant. Fluid spaces are present (asterisk) within the organ of Corti, although no intact inner or outer hair cells can be identified. T, tectorial membrane. Bar, 50 μm.

We tested the mice between 18 and 24 days postnatal, since this represents a time period during which the mouse inner ear matures to achieve adult hearing sensitivity. Results from one such evaluation are shown in Figure 3. ABR recordings indicated that the mice displaying the circling phenotype were totally deaf at all

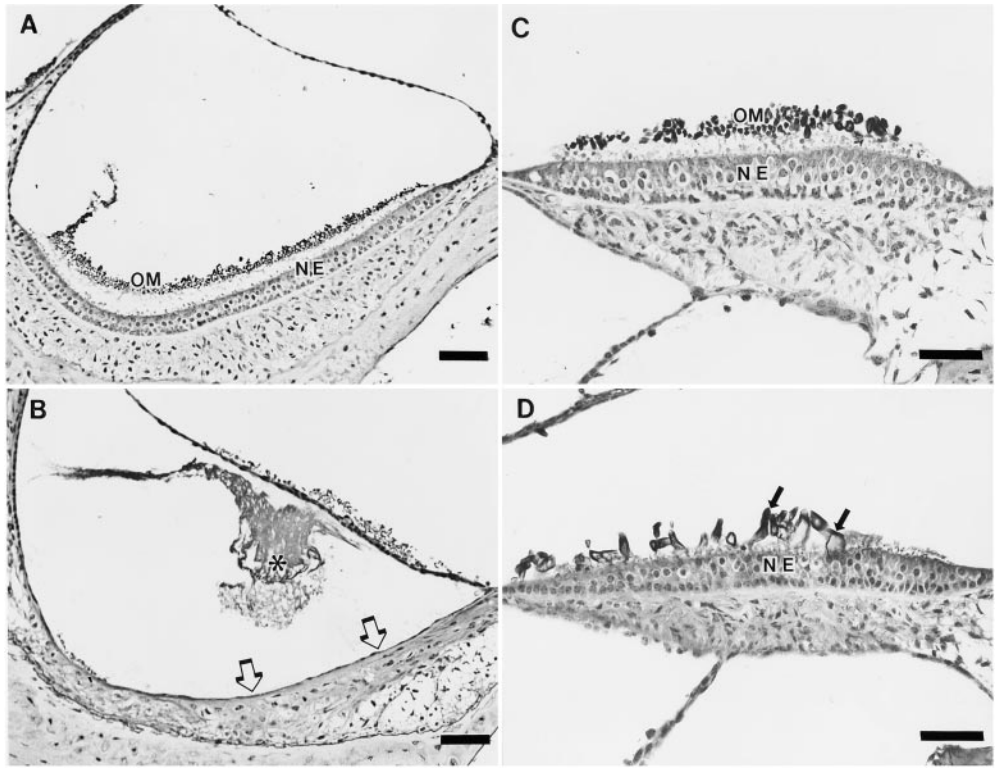


Figure 2.—Morphology of the saccule and utricle from normal and *TgN2742Rpw* mutant mice at ~1 yr of age. (A) Saccule from a normal mouse showing the neuroepithelium (NE) with overlying otoconial membrane (OM). Bar, 50 μm. (B) Saccule from a *TgN2742Rpw* mutant showing absence of neuro-epithelium (arrows). A remnant of the degenerated otoconial membrane is seen within the saccular cavity (asterisk). Bar, 50 μm. (C) Utricular neuroepithelium (NE) and its otoconial membrane (OM) from a normal mouse. Bar, 50 μm. (D) Utricular neuroepithelium (NE) from a *TgN2742Rpw* mutant. The crystalline layer of the otoconial membrane is composed of sparsely distributed, abnormally large otoconia (arrows). Bar, 50 μm.

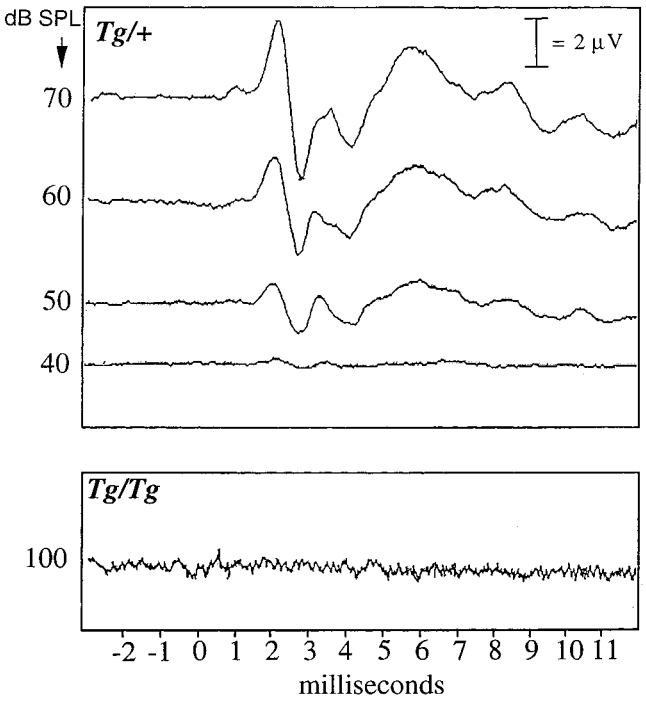


Figure 3.—Representative ABR waveforms from *TgN2742Rpw*/+ (Tg/+) and *TgN2742Rpw*/*TgN2742Rpw* (Tg/Tg) adult mice in response to a click stimulus. Characteristic waveform (five peaks) was obtained for *TgN2742Rpw*/+ mice at the various intensities tested (40–70 dB), while no response was elicited for *TgN2742Rpw*/*TgN2742Rpw* mice even at 100 dB. The stimulus was initiated at time 0 (*x* axis) and the ABR waveforms were detected within 5–7 msec. Amplitude (along the *y* axis) scale bars are indicated on the right (in microvolts).

frequencies tested; the noncircling siblings, whether they were wild type or heterozygous for the mutation, had thresholds in the normal range. Mutant mice older than 3.5 wk also showed no signs of auditory function (data not shown).

To test for vestibular dysfunction in the *TgN2742Rpw* mutant mice, we conducted swimming tests. Mice from three litters derived from heterozygous parents were tested at 24–30 days of age. A total of 9 wild-type (+/+), 15 heterozygous (*TgN2742Rpw*/+), and 8 homozygous (*TgN2742Rpw*/*TgN2742Rpw*) mice were tested. All the +/+ and *TgN2742Rpw*/+ mice displayed normal swimming behavior resulting in proper orientation of the mice with respect to the water surface (see materials and methods). However, all of the *TgN2742Rpw*/*TgN2742Rpw* mice showed abnormal swimming behavior associated with lack of orientation: when placed in water, the mutants spiraled underwater (in a corkscrew fashion) unable to maintain their noses and tails above the water surface. Mutants needed to be rescued promptly to prevent drowning.

**Cloning the mutant locus:** To characterize the mutation in the *TgN2742Rpw* line at the molecular level, we cloned and analyzed both the mutant locus and the corresponding wild-type region. For this purpose, a genomic cosmid library was prepared from the *TgN2742Rpw* mutant mice and screened using a plasmid rescue procedure that was originally used for cloning the *limb deformity* locus (Woychik *et al.*1985; see materials and methods for details). The cosmid clones obtained were screened for the presence of mouse genomic DNA flanking the transgene insertion site. One such clone, cosmid-9, contained ~25 kb of mouse genomic DNA in addition to approximately three copies of the transgene (≈20 kb) (Figure 4A). Within the 25 kb of mouse genomic DNA on cosmid-9, we identified a unique copy fragment, F9 (Figure 4A), and used this fragment as a probe to detect a restriction fragment length polymorphism (RFLP) associated with the mutant allele. To accomplish this, F9 was hybridized to Southern blots of restriction-enzyme-digested wild type, heterozygous, and homozygous DNA that had been resolved by pulsed-field gel electrophoresis. We used restriction enzymes that cut within the transgene (such as *Sal*I) as well as enzymes that do not cut within the transgene (such as *Sfi*I). In both cases, we were able to detect a unique RFLP in DNA containing the mutant allele (Figure 4, B and C). Therefore, the F9 probe corresponds to the region flanking the transgene insertion site. Furthermore, data from the *Sfi*I restriction analysis suggest that ~30 copies of the transgene are present at the site of insertion (Figure 4, B and C).

To further characterize the mutant locus, a wild-type BAC mouse genomic library was screened using the F9 sequence as a probe. Three clones were isolated with an average insert size of 110 kb. One of these clones (BAC36) spans the transgene insertion site on the *TgN2742Rpw* mutant allele (Figure 4A). We made this determination by utilizing end-clones derived from the insert DNA contained in the BAC36 (labeled "A" and "B" in Figure 4A) as probes on Southern blots containing genomic DNA digested with an enzyme that cuts within the inserted transgene DNA (*Sal*I). The genomic DNA samples that were used for this experiment were prepared from mice that were either wild type, heterozygous, or homozygous for the *TgN2742Rpw* mutation. Analysis of the data revealed that end-clones A and B hybridize to the same-sized *Sal*I fragment (680 kb) in the wild-type DNA, but each hybridized to a unique *Sal*I fragment in the mutant allele; *i.e.*, end-clone A hybridizes with a 415-kb fragment, and end-clone B hybridized with a 375-kb fragment (Figure 4D). The fact that both end-clones hybridize to the mutant DNA indicates that there is not a large deletion (>110 kb, the size of the BAC) associated with the transgene insertion site.

**Mapping the *TgN2742Rpw* mutant locus:** To localize the *TgN2742Rpw* transgene insertion site on the genetic map, we used a 4.5-kb *Eco*RI fragment from the region flanking the transgene insertion as a probe to analyze DNA from a previously described *M. musculus* × *M.*

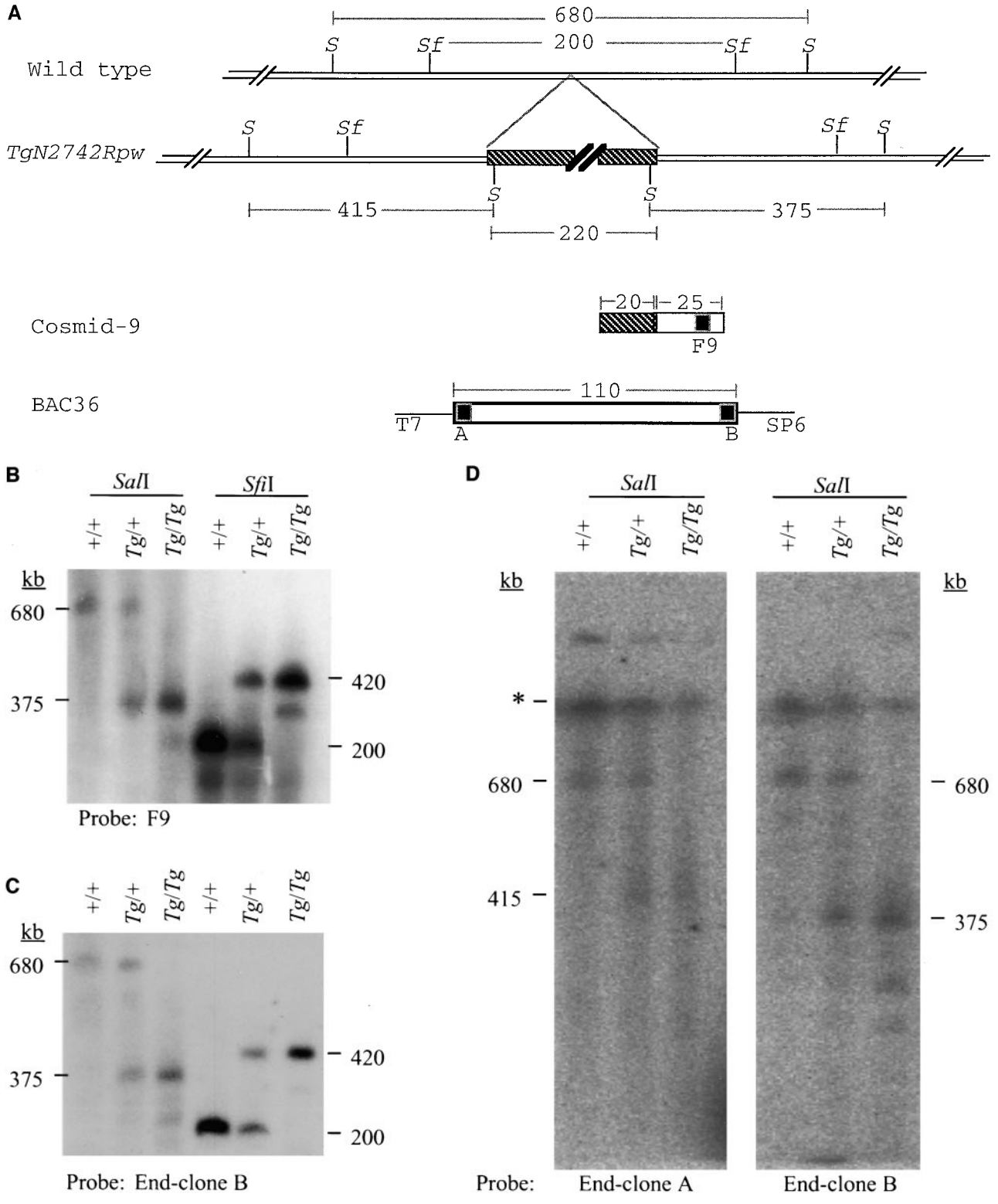


Figure 4.—Characterization of the *TgN2742Rpw* mutant locus. (A) Gross physical map of the mutant locus in the *TgN2742Rpw* line and its corresponding wild-type region based on pulsed-field gel electrophoresis. The inserted transgene DNA is designated as a hatched box. The unique sequence fragments [F9, end-clone A (represented by letter "A"), and end-clone B (represented by letter "B")] used as probes are shown as black boxes. Numbers refer to DNA fragment sizes in kilobases. Figure not to scale to show structure of clones. Precise end points of the BAC clone have not been determined, and the *Sal*I sites have not been mapped with respect to the *Sfi*I sites. Restriction sites: S, *Sal*I; Sf, *Sfi*I. (B–D) Southern blots of spleen DNA from wild-type (+/+), *TgN2742Rpw*/+ (Tg/+), and *TgN2742Rpw*/*TgN2742Rpw* (Tg/Tg) mice digested with *Sal*I or *Sfi*I and separated at constant temperature (11°) in a gel run in a CHEF Mapper PFGE unit (Bio-Rad, Richmond, CA) on an auto-algorithm setting specified to separate fragments 50 to 1500 kb (B and C) or 30 to 800 kb (D). Probes representing sequence fragment F9 from

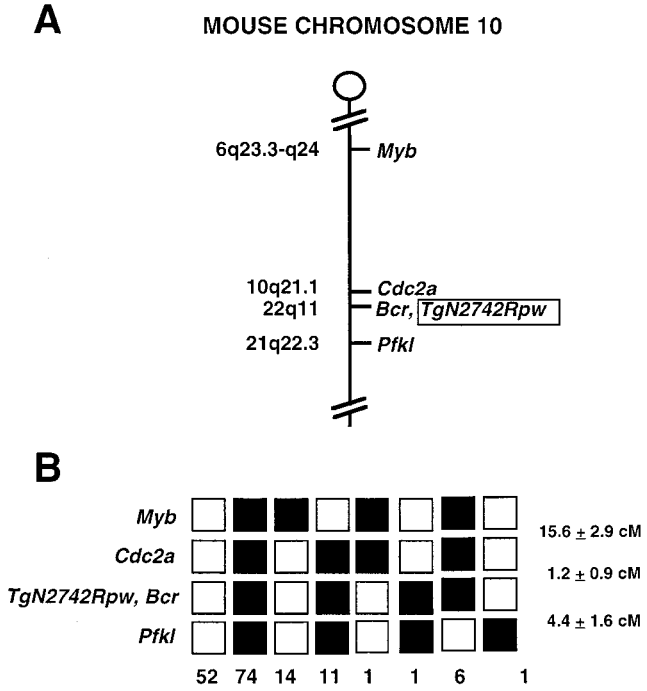


Figure 5.—Map location of *TgN2742Rpw* mutation. (A) Partial map of mouse chromosome 10 showing the position of the *TgN2742Rpw* insertion site relative to other Mmu10 genes. The positions of human homologues of *Myb*, *Cdc2a*, *Bcr*, and *Pfkl* are shown to the left of the map in the upper portion of the figure. (B) Summary of the distribution of *M. spretus* or *M. musculus* (C3Hf/Rl) alleles detected by *Myb*, *Cdc2a*, *Bcr*, *TgN2742Rpw*, and *Pfkl* probes in 160 IB progeny. Each column of boxes represents a type of parental or recombinant chromosome; the number of backcross mice inheriting a particular type of chromosome are listed at the bottom of each column. White boxes represent the inheritance of a C3Hf/Rl allele for a gene, while black boxes denote the presence of *M. spretus* alleles. Recombination distances calculated from these data, given in centimorgans (cM) with standard errors, are shown at right between rows representing adjacent genes.

*spretus* interspecific backcross (see materials and methods). The segregation pattern detected by the 4.5-kb probe was compared to those of more than 450 markers that had been mapped previously in the same IB system (L. Stubbs, unpublished results). These studies mapped the transgene insertion site to the central portion of mouse chromosome 10, located just distal to the gene encoding cell division cycle control protein 2a (*Cdc2a*; located within 0.1–5.8 cM of that gene at 99% confidence limits, as computed by Map Manager software). The 4.5-kb fragment cosegregated with the conserved breakpoint cluster region gene *Bcr* (Figure 5), indicating that *Bcr* and the *TgN2742Rpw* insertion sites are tightly linked on mouse chromosome 10 (within 0–2.9 cM at 99% confidence limits).

## DISCUSSION

**A new mouse mutation with inner ear defects:** We have identified a new mouse mutation that causes deafness and balance disorders associated with morphological defects of the inner ear. Phenotypic characterization of the mutant mice revealed characteristic changes in the neuroepithelium of the inner ear. Additionally, investigation of the hearing function using the ABR procedure showed that the *TgN2742Rpw* mutation causes total deafness. Since the mutants are deaf at all frequencies tested, it appears that the defect is not restricted to a particular region of the cochlea that is responsive to specific sound frequencies. Our histological examination of inner ears from adult mutants revealed nearly complete absence of the organ of Corti together with loss of spiral ganglion cells in the cochlea. In addition, there is loss of the neuroepithelium of the saccule, together with an occasional malformation of the otoconia overlying the utricular macula. These abnormalities are sufficiently severe to account for the auditory and vestibular deficits observed during functional testing of the mice.

Although there is virtually a complete loss of the cochlear neuroepithelium in the mutant mice, the stria vascularis appears essentially normal and there is no evidence of reduced fluid volume in the cochlear duct or saccule. The inner ear pathology is, therefore, different from that found in the cochleo-saccular mutants, which show strial degeneration and collapse of the membranous walls of the labyrinth. In cochleo-saccular mutants, such as the *dominant spotting (W)* or *Steel (Sl)* mice (Steel 1995), degeneration of the organ of Corti occurs as a consequence of disturbed inner ear fluid homeostasis resulting from dysfunction of the stria vascularis. In our *TgN2742Rpw* mutant line, the mutation appears to have a direct effect on the neuroepithelia of the cochlea and the saccule. Therefore, the phenotype in the *TgN2742Rpw* mutant is not a secondary consequence of defects in the stria vascularis.

The fact that remnants of the organ of Corti are present in the adult mutant mice suggests that the cochlear structures may develop in a relatively normal fashion and then undergo degeneration sometime after birth. Morphological studies on inner ear tissues taken at closely spaced intervals after the time of birth are currently under way to determine the extent of early development of the neuroepithelia and to characterize

cosmid-9 (B) and end-clone B (C) and end-clones A and B (D) from BAC36 were hybridized to the Southern blots. Numbers refer to DNA fragment sizes in kilobases. Asterisk represents the limiting mobility zone; artificial bands appear in this zone due to aggregation of high-molecular-weight DNA (>800 kb).

the sequence of degenerative changes leading to the abnormalities observed in the adult mutant mice. These studies should provide valuable insights into the developmental origin of the inner ear defects in the *TgN2742Rpw* mutant line and should allow a more detailed phenotypic comparison of this mutant with other previously described mice having mutations of the neuroepithelial type.

Thus far our light microscopic observations in adult animals indicate that degenerative changes of the inner ear sensory epithelia in *TgN2742Rpw* mutants are limited to the cochlea and saccule, and that there are no obvious abnormalities of the neuroepithelia of the utricle and semicircular ducts. This pattern of morphological defects has also been reported to occur in several other neuroepithelial mutants such as *shaker-2*, *pirouette*, *waltzer*, and *spinner* (Deol 1968). However, recent studies based on electron and laser confocal microscopy have revealed more widespread involvement of the vestibular apparatus in some of these mutants (Raphael *et al.* 1999). We are currently pursuing electron microscopic work to supplement our light microscopic studies in an effort to determine whether ultrastructural defects may also be present in the utricular macula and semicircular duct cristae of the *TgN2742Rpw* mutants.

The advantage of using an insertional mutation to isolate a new gene is that the mutant locus is "tagged" by the integrated DNA sequences and therefore can be cloned without having to resort to standard positional cloning techniques. One potential problem with insertional mutations generated by the pronuclear microinjection procedure is that there can be large deletions associated with the mutant locus (Singh *et al.* 1991; Rijkers *et al.* 1994). Large deletions at the transgene insertion site can complicate efforts to identify the gene that is directly associated with the mutant phenotype. The data we describe here suggest that there has not been a large deletion of DNA at the site of transgene integration in the *TgN2742Rpw* line. The fact that we have isolated a wild-type BAC clone that spans the transgene integration site should position us to find the gene that is directly associated with the mutant phenotype in this line.

The region to which the *TgN2742Rpw* insertion has been mapped contains several other mouse mutations that affect the function and development of the inner ear. The recently published chromosome 10 committee report places *Bcr* and *Cdc2a* at 40 and 38.0 cM from the Mmu10 centromere, respectively, which positions these two genes near the *TgN2742Rpw* mutation and three previously identified inner ear mutations, namely, Ames Waltzer (*av*, 37 cM), Jackson circler (*jc*, 33 cM), and Waltzer (*v*, 30 cM). Given the margins of error associated with these consensus map positions, it is possible that the *TgN2742Rpw* mutation is allelic with one of these three existing mutations.

Although mouse *Cdc2a* and *Bcr* genes are located very close together, the homologues of these two genes are not linked in the human genome. The human counterpart of *Cdc2a*, *CDC2*, has been mapped to human chromosome 10q21 (Nazarenko *et al.* 1991), while *BCR* is located on chromosome 22q11 (Shtivelman *et al.* 1985). Genes located <1 cM distal from Bcr are related to sequences located on human chromosome 21q22.3, suggesting that the 22q11/Mmu10 homology region is relatively small (Burmeister *et al.* 1998). It is therefore difficult to predict whether human sequences related to the *TgN2742Rpw* mutation will be found in chromosomes 10q21, 22q11, or 21q22.3.

Some potentially interesting connections between the *TgN2742Rpw* phenotype and a human deafness locus mapped to chromosome 10 are noteworthy. This deafness mutation, *DFNB12*, has similar features with *TgN2742Rpw* and has recently been mapped to 10q21-q22 (Chaib 1996). Mutations in the *DFNB12* locus are associated with a recessive nonsyndromic deafness marked by a profound prelingual sensorineural hearing defect. *DFNB12* has been proposed to possibly represent the human homologue of the murine *jc*, *av*, or *v* mutations (Petit 1996). This raises the possibility that there may be a connection between the *TgN2742Rpw* and *DFNB12* mutations.

Mutations that affect the sensory neuroepithelia are a major cause of inner ear defects in humans. Given the importance of this type of pathology in humans, the transgenic line *TgN2742Rpw* may prove to be very useful as a model to study sensorineural deafness, and specifically, to help in the identification of gene(s) essential for normal structure and function of the inner ear.

We thank Crystal Rohrbaugh, and Drs. Noel Murcia, Mitch Klebig, and Scott Bultman for critical reading of the manuscript. The authors are grateful to Karen S. Pawlowski for histological processing of the inner ear tissues utilized in this study. This research was supported by National Institute on Deafness and Other Communication Disorders Grant 1RO1-DC03420 to R.P.W. and by the U.S. Department of Energy under contract W-7405-Eng-48 with the University of California, Lawrence Livermore National Laboratory, for L.S. and under contract DE-AC05-960R22464 with Lockheed Martin Energy Research, for N.L.A.C.

## LITERATURE CITED

Ausubel, F. M., R. Brent, R. E. Kingston, D. D. Moore, J. G. Seidman *et al.*, 1991 *Current Protocols in Molecular Biology*. Greene Publishing Associates and Wiley-Interscience, New York.

Avraham, K. B., T. Hasson, K. P. Steel, D. M. Kingsley, L. B. Russell *et al.*, 1995 The mouse *Snell's waltzer* deafness gene encodes an unconventional myosin required for structural integrity of inner ear hair cells. Nat. Genet. **11:** 369–375.

Bates, P. F., and Swift, R. A. 1983 Double cos site vectors: simplified cosmid cloning. Gene **26:** 137–146.

Bouguski, M. S., T. M. Lowe and C. M. Tolstoshev, 1993 dbEST—database for expressed sequence tags. Nat. Genet. **4:** 332–333.

Burmeister, M., E. C. Bryda, J. F. Bureau and K. Noben-Trauth, 1998 Encyclopedia of the mouse genome VII. Mouse chromosome 10. Mamm. Genome **8:** Spec No. S200-14.

Chaib, H., C. Place, N. Salem, C. Dode, S. Chardenoux *et al.*, 1996 Mapping of *DFNB12*, a gene for a non-syndromal auto-

somal recessive deafness, to chromosome 10q21-22. Hum. Mol. Genet. **5:** 1061–1064.

Deol, M. S., 1968 Inherited disease of the inner ear in man in the light of studies on the mouse. J. Med. Genet. **5:** 137–158.

Erway, L., J. Willott, J. Archer and D. Harrison, 1993 Genetics of age-related hearing loss in mice: I. Inbred and F1 hybrid strains. Hear. Res. **65:** 125–132.

Fraser, G. R., 1976 *The Causes of Profound Deafness in Childhood.* Johns Hopkins University Press, Baltimore.

Gibson, F., J. Walsh, P. Mburu, A. Varela, K. A. Brown *et al.*, 1995 A type VII myosin encoded by the mouse deafness gene shaker-1. Nature **374:** 62–64.

Gordon, J. 1992 Standardized nomenclature for transgenic animals. ILAR News **34:** 45.

Kalatzis, V., and C. Petit, 1998 The fundamental and medical impacts of recent progress in research on hereditary hearing loss. Hum. Mol. Gen. **7:** 1589–1597.

Levanon, D., E. Danciger, N. Dafni, Y. Bernstein, A. Elson *et al.*, 1989 The primary structure of human liver type phosphofructokinase and its comparison with other types of PFK. DNA **8:** 733–743.

Liu, X. Z., J. Walsh, Y. Tamagawa, K. Kitamura, M. Nishizawa *et al.*, 1997 Mutation in the myosin VIIA gene causes non-syndromic recessive deafness. Nat. Genet. **16:** 188–190.

Manly, K. F., 1993 A Macintosh program for storage and analysis of experimental genetic mapping data. Mamm. Genome **4:** 303–313.

Morton, N. E. 1991 Genetic epidemiology of hearing impairment. Ann. NY Acad. Sci. **630:** 16–31.

Mucenski, M. L., K. McLain, A. B. Kier, S. H. Swerdlow, C. M. Schreiner *et al.*, 1991 A functional c-myb gene is required for normal murine fetal hepatic hematopoiesis. Cell **65:** 677–689.

Nadeau, J. H., M. Kosowsky and K. P. Steel, 1991 Comparative gene mapping, genome duplication, and the genetics of hearing. Ann. NY Acad. Sci. **630:** 49–67.

Nazarenko, S. A., N. V. Ostroverhova and N. K. Spurr, 1991 Regional assignment of the human cell cycle control gene CDC2 to chromosome 10q21 by in situ hybridization. Hum. Genet. **87:** 621–622.

Petit, C. 1996 Genes responsible for human hereditary deafness: symphony of a thousand. Nat. Genet. **14:** 385–391.

Probst, F. J., R. A. Fridell, Y. Raphael, T. L. Saunders, A. Wang *et al.*, 1998 Correction of deafness in shaker-2 mice by an unconventional myosin in a BAC transgene. Science **280:** 1444–1447.

Raphael, Y., D. C. Kohrman, F. J. Probst, E. Lambert, L. Beyer *et al.*, 1999 The cytocaud: actin filaments on the loose. Abstracts of the 22nd. Midwinter Meeting of the Association for Research in Otolaryngology, p. 8.

Rijkers, T., A. Peetz and U. Ruther, 1994 Insertional mutagenesis in transgenic mice. Transgenic Res. **3:** 203–215.

Sambrook, J., E. F. Fritsch and T. Maniatis, 1989 *Molecular Cloning: A Laboratory Manual.* Cold Spring Harbor Laboratory Press, Cold Spring Harbor, NY.

Schuknecht, H. F. 1993 Developmental defects, pp. 115–189 in *Pathology of the Ear,* edited by R. K. Bussey, T. Lazar and F. M. Klass. Lea & Febiger, Philadelphia.

Shtivelman, E., B. Lifshitz, R. P. Gale and E. Canaani, 1985 Fused transcript of abl and bcr genes in chronic myelogenous leukaemia. Nature **315:** 550–554.

Singh, G., D. M. Supp, C. Schreiner, J. McNeish, H.-J. Merker *et al.*, 1991 *legless* insertional mutation: morphological, molecular, and genetic characterization. Genes Dev. **5:** 2245–2255.

Steel, K. P. 1995 Inherited hearing defects in mice. Annu. Rev. Genet. **29:** 675–701.

Stubbs, L., A. Poustka, A. Baron, H. Lehrach, P. Lonai *et al.*, 1990 The murine genes Hox-5.1 and Hox-4.1 belong to the same HOX complex on chromosome 2. Genomics **7:** 422–427.

Stubbs, L., E. M. Rinchik, E. Goldberg, B. Rudy, M. A. Handel *et al.*, 1994 Clustering of six human 11p15 gene homologs within a 500-kb interval of proximal mouse chromosome 7. Genomics **24:** 324–332.

Stubbs, L., L. Chittenden, A. Chakrabarti and E. Onaivi, 1996 The gene encoding the central cannabinoid receptor is located in proximal mouse Chromosome 4. Mamm. Genome **7:** 165–166.

Van Camp, G., and R. J. H. Smith Hereditary hearing loss homepage. World Wide Web URL: http://dnalab-www.uia.ac.be/dnalab/hhh/.

Wang, A., Y. Liang, R. A. Fridell, F. J. Probst, E. R. Wilcox *et al.*, 1998 Association of unconventional myosin MYO15 mutations with human nonsyndromic deafness DFNB3. Science **280:** 1447–1451.

Weil, D., S. Blanchard, J. Kaplan, P. Guilford, F. Gibson *et al.*, 1995 Defective myosin VIIA gene responsible for Usher syndrome type 1B. Nature **374:** 60–61.

Weil, D., P. Kussel, S. Blanchard, G. Levy, F. Levi-Acobas *et al.*, 1997 The autosomal recessive isolated deafness, DFNB2, and the Usher 1B syndrome are allelic defects of the myosin-VIIA gene. Nat. Genet. **16:** 191–193.

Woychik, R. P., T. A. Stewart, L. G. Davis, P. D'Eustachio and P. Leder, 1985 An inherited limb deformity created by insertional mutagenesis in a transgenic mouse. Nature **318:** 36–40.

Communicating editor: N. A. Jenkins